Research Article | Vol. 27, No. 6 | 18 Mar 2019 | OPTICS EXPRESS 9155
Optics EXPRESS

Enhanced optical frequency comb generation by pulsed gain-switching of optically injected semiconductor lasers

A. Rosado,[1,*] A. Pérez-Serrano,[1] J. M. G. Tijero,[1] Á. Valle,[2] L. Pesquera,[2] and I. Esquivias[1]

[1] CEMDATIC - E.T.S.I Telecomunicación, Universidad Politécnica de Madrid (UPM), 28040 Madrid, Spain
[2] Instituto de Física de Cantabria, (CSIC-Universidad de Cantabria), 39005 Santander, Spain
[*] alejandro.rosado@upm.es

Abstract: We report on the experimental generation of broad and flat optical frequency combs (OFC) in a 1550 nm laser diode using gain switching with pulsed electrical excitation together with optical injection. The combination of both techniques allows the generation of high-quality OFCs at a repetition frequency of 500 MHz, showing a low-noise optical spectrum with unprecedent features in terms of width (108 tones within 10 dB) and flatness (56 tones within 3 dB) in comparison with those previously reported for this modulation frequency. The influence of the injection conditions on the OFC quality is studied. Using these two techniques, it has been possible to reduce the separation between tones, generating high spectral performance OFCs with a repetition rate of 100 MHz.

© 2019 Optical Society of America under the terms of the OSA Open Access Publishing Agreement

1. Introduction

In the same way as for other photonic technologies, the use of semiconductor sources for the generation of optical frequency combs (OFCs) is gaining increasing relevance due to the inherent advantages of the laser diodes in terms of high efficiency, low cost and small footprint, thus allowing to envisage prospects for the deployment of the technology outside the laboratory at a cost-effective price [1–3].

Gain-switching (GS) has proven its convenience as a method for generating OFCs due to its easy implementation, robustness and stability, controllable repetition rate, and adaptability for integration using generic platforms [4–6]. OFCs generated by GS have found applications mainly in optical communications [1,7] but also in sub-terahertz generation [8] and more recently in absorption spectroscopy [9, 10]. The usual implementation of the GS technique for the generation of OFCs consists in driving the laser with the superposition of a direct bias current and a radio-frequency (RF) sinusoidal current. The frequency and amplitude of the RF current, in combination with the bias current are the key parameters of the process. In this context, the usual practice is to include under the term gain-switching any large signal modulation process, even though the laser may not actually be switched-off but just modulated. We have recently provided a systematic analysis of the effects of these switching conditions in the characteristics of the generated OFCs [11]. In simple terms, for repetition frequencies (roughly ~ 5-25 GHz) of the order of the frequency of the relaxation oscillations, there is a relatively wide range of driving conditions for exciting only the first spike of the relaxation oscillations before the laser emission drops down to a minimum level for a time short enough as to guarantee the preservation of the coherence of the subsequent pulses, thus resulting in a broad spectrum with discernible spectral lines. However, as detailed later in section 3, for low repetition frequencies ($\lesssim$ 1 GHz) the range of driving conditions for getting broad and well resolved combs is very small. Out of this small range either the pulses are spectrally narrow when the laser is just modulated, or there is a switch-off period long enough for the coherence to be lost, resulting in a spectrum without

#355860 https://doi.org/10.1364/OE.27.009155
Journal © 2019 Received 20 Dec 2018; revised 21 Feb 2019; accepted 28 Feb 2019; published 14 Mar 2019

Optics EXPRESS

discernible lines.

And yet, it is in this low repetition frequency range where OFCs generated by GS have recently found interesting advantages in dual-comb optical spectroscopy [9]. These advantages are simplicity of use, control of the line spacing, compactness and potential for integration, and capabilities for implementation outside the 1.5 μm spectral range. Obviously, these advantages can only be fully exploited if the number of spectral lines of the OFC and the separation between them can sustain the high resolution in a sufficiently broad spectral range which is characteristic of dual-comb spectroscopy. The authors in [9] illustrate the potential of their approach with the OFC generated by a 1 GHz sinusoidal RF current. In order to get a comb with enough number of lines, they had to make a meticulous optimization of the switching and optical injection conditions. However, when higher resolution (lower repetition frequency) is required the approach is clearly hindered by the narrowing of the window of suitable conditions for the required spectral width of the comb, thus compromising the usefulness of the OFCs generated by GS for this application.

On the other hand, since the early times of GS, not only sinusoidal RF excitation but also pulsed excitation conditions, either with or without a dc component, have been regularly used for generating short optical pulses at a wide range of wavelengths and repetition frequencies [12–16]. Although the spectral width of the trains of pulses generated by pulsed GS has been analyzed and manipulated [13, 17, 18], the coherence between pulses and their potential as OFCs has not been studied. Taking into account that the coherence relies on the preservation of stimulated emission during the switch-off period as a seed out of which to build up the next pulse [11, 19], a poor coherence is expected from low repetition frequency trains of pulses having long switch-off periods between them.

Concurrently, optical injection (OI) of a slave gain-switched laser by a master laser has demonstrated to improve the quality of the OFC by driving the slave to emit with the optical characteristics inherited from the master [20–22]. In particular, it has been claimed that the master laser can seed the slave during the switch-off periods with the stimulated emission out of which to build up the next pulse, thus preserving the coherence of the train of pulses [11, 19].

In this paper, we put together these two concepts, first, the generation of spectrally broad and incoherent trains of short optical pulses by pulsed GS and second, the improvement of the coherence of such pulses by optical injection. By this method, we experimentally demonstrate for the first time to the best of our knowledge the direct generation by GS of broad OFCs, containing an unprecedent number of well resolved spectral lines separated by repetition frequencies lower than 1 GHz, without further expansion stages. Moreover, we perform an analysis of the effects of the GS and OI conditions on the quality of the OFCs. The findings reported in this paper are a significant step forward in the direction of extending the performance range of the OFCs generated by GS to lower frequencies, while keeping simplicity as the distinct feature of the GS method. They may contribute to facilitate the application of GS to dual-comb spectroscopy and other applications requiring the direct generation by a simple method of relatively wide combs at low separation frequencies.

2. Experimental setup

The experimental setup is shown in Fig. 1. The OFCs were generated by GS a high frequency single-frequency laser diode. The device, a discrete mode laser (DML) (Eblana Photonics EP1550- 0-DM-H19-FM) is based on a multi-quantum well structure in a ridge waveguide with index perturbations, in order to allow single-frequency emission [23]. The threshold current of this laser is I_{th} = 14.8 mA with a nominal modulation bandwidth of 10 GHz. More details can be found in [11]. This laser has no built-in optical isolator in order to allow external optical injection. The laser was driven by the superposition of two electrical signals: a bias current (I_{bias}), provided by a current source (Arroyo 4205) and either i) a sinusoidal signal provided by a microwave/RF generator (Rohde & Schwarz SMB100A) or ii) a low duty cycle square signal

Optics EXPRESS

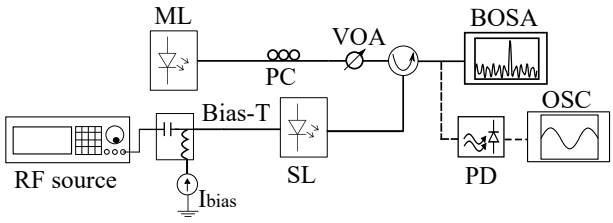

Fig. 1. Schematics of the experimental setup. ML: master laser, SL: slave laser, PC: polarization controller, VOA: variable optical attenuator, PD: photodetector, OSC: oscilloscope, BOSA: Brillouin optical spectrum analyzer.

provided by a pulse pattern generator (Anritsu MU181020A) operating at bit rates up to 12.5 Gb/s. For the OI experiments, an optical circulator was used to inject the output power from a narrow linewidth tunable laser (Pure Photonics PPCL300) acting as master laser (ML) into the gain-switched DML, operating as slave laser (SL). A polarization controller was used to maximize the coupling between both lasers. Additional details on the CW and high-frequency properties of this particular DML can be found in [11]. The output power was spectrally characterized by means of a high resolution (10 MHz) Brillouin optical spectrum analyzer (BOSA) (Aragon Photonics BOSA 210). A digital signal analyzer (Tektronix DSA8200), equipped with a 20 GHz bandwidth optical input module, was employed to measure the temporal profiles of the optical pulses. The temporal profiles were averaged 20 times. The quality of the OFCs was characterized by means of the 10 dB spectral width (δf_{10}) and the carrier-to-noise ratio (CNR) as defined in [11].

3. Results and discussion

In the time domain broad OFCs with well resolved tones implies trains of short optical pulses with a high degree of coherence between them. However, as we reported in [11] at low repetition frequencies (f_R = 500 MHz), broad, flat and well resolved OFCs cannot be generated by GS under sinusoidal electrical excitation and only relatively narrow and non-flat OFCs are generated when the laser is not actually switched-off, i.e., under direct modulation conditions. An example of this behaviour is illustrated in Fig. 2 for f_R = 500 MHz. The estimated temporal profile of the injected current is shown in Fig. 2(a). The measured temporal profile of the output power and the corresponding measured optical spectrum are shown in Figs. 2(b) and 2(c), respectively. We estimate the temporal profile of the current as:

$$i(t) = \frac{2V_{\mathrm{RF}}}{Z_0 + Z_L}\cos(2\pi f_R t) + I_{bias}, \tag{1}$$

where V_{RF} is the voltage amplitude at the electrical input of the laser, Z_0 = 50 Ω is the internal impedance of the RF source and Z_L is the laser impedance. In a separate set-up, the impedance of the laser module was measured as a function of the frequency with a vector network analyzer, yielding a value close to 50 Ω at frequencies lower than 5 GHz. Under these excitation conditions (I_{bias} = 68 mA, V_{RF} = 2.4 V), the injected current is always above threshold current (14.8 mA), which is indicated by the dashed red line in Fig. 2(a). In consequence, the laser is always on and the emitted optical power shows a sinusoidal temporal profile (Fig. 2(b)). The generated OFC (Fig. 2(c)) shows clearly defined tones of unequal amplitudes. The carrier-to-noise ratio and the 10 dB spectral width are CNR = 43 dB and δf_{10} = 10 GHz, corresponding to 9 comb lines. The flatness of the OFC is poor, as several lines are clearly depressed. The shape of the spectrum has been attributed in [11] to a combination of amplitude modulation and frequency modulation caused by the adiabatic chirp.

Optics EXPRESS

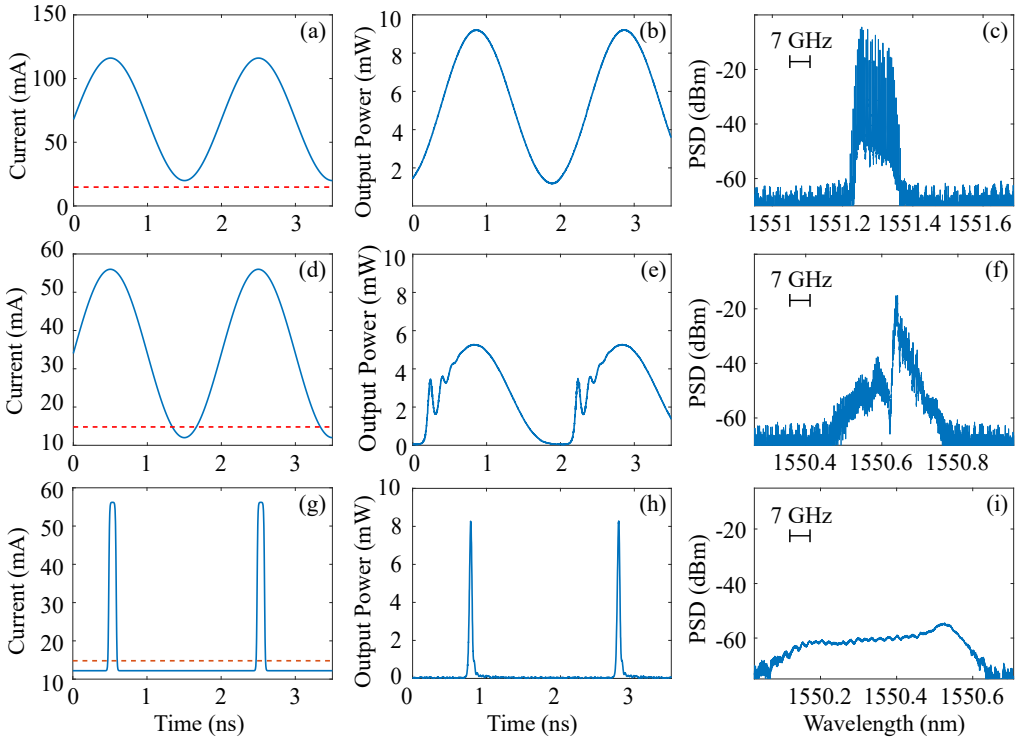

Fig. 2. Temporal and spectral characteristics of the emission of the gain-switched laser when driven at 500 MHz under the following driving conditions: upper row (a)-(c), sinusoidal excitation with I_{bias} = 68 mA and V_{RF} = 2.4 V; middle row (d)-(f), sinusoidal excitation with I_{bias} = 34 mA and V_{RF} = 1.1 V; bottom row (g)-(i), pulsed excitation with I_{OFF} = 12.2 mA and I_{ON} = 56.2 mA. (a), (d) and (g) show the estimated temporal profiles of the injected current (see text for details). The dashed red lines indicate the threshold current.

When at f_R = 500 MHz sinusoidal driving conditions are set up for obtaining trains of GS pulses separated by switch-off periods (Fig. 2(d)), the profile of the generated pulses looks like the one plotted in Fig. 2(e) for I_{bias} = 34 mA and V_{RF} = 1.1 V. Since the injected current lies below threshold for a fraction of the cycle, an initial spike corresponding to GS is clearly seen at the onset of the pulse. However, this initial spike is followed by a sinusoidal-like profile in which oscillations, at a frequency matching the relaxation oscillations frequency at this injection level, are clearly seen. From these long pulses separated by relatively large switch-off periods, broad and well resolved OFCs are not expected and this is indeed what Fig. 2(f) evidences. It is clear at this point that in order to produce at these low frequencies trains of short optical pulses by GS, the electrical excitation should also be a pulse train with an amplitude and duration enough to excite the first relaxation oscillation spike. Figs. 2(g)-2(i) show respectively the estimated profile of the electrical excitation pulses, the temporal profile of the optical pulses and the corresponding optical spectrum, resulting of such an excitation regime. In this case, the electrical pulse of a width τ_{elec} = 100 ps switches the injection current between a value below threshold I_{OFF} = 12.2 mA and a value above threshold I_{ON} = 56.2 mA. I_{OFF} and I_{ON} are estimated from I_{bias}, V_{RF} and the duty cycle ($f_R\tau_{elec}$) according to:

$$I_{OFF} = I_{bias} - \frac{4V_{RF}}{Z_0 + Z_L} f_R \tau_{elec} \quad \text{and} \quad I_{ON} = I_{OFF} + \frac{4V_{RF}}{Z_0 + Z_L}. \tag{2}$$

Optics EXPRESS

The train of the generated optical pulses is shown in Fig. 2(h). The full-width half-maximum (FWHM) of the pulses is Δt = 40 ps. As expected from such short pulses the corresponding optical spectrum (Fig. 2(i)) is much broader (~ 50 GHz) than previous ones. However the spectrum is still continuous and does not show the clearly discernible peaks characteristic of an OFC. This fact should be attributed to the lack of coherence between pulses: as the laser is completely switched off between pulses, each new pulse builds up from spontaneously emitted photons with random initial phase and therefore their optical fields do not add up coherently resulting in the absence of discrete spectral lines. The RF spectrum (not shown) exhibits narrow harmonics with low noise floor as a consequence of the periodicity of the optical intensity. In this pulsed regime we made a detailed exploration of the electrical injection conditions required for obtaining OFCs and found out that even with I_{OFF} close to I_{th} no OFC are generated.

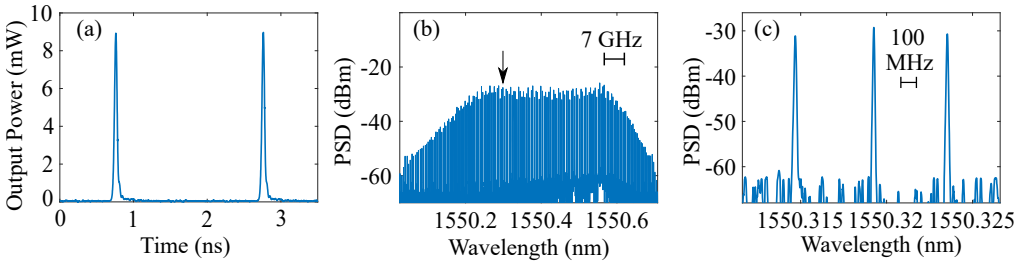

Fig. 3. Temporal trace of the output power (a) and optical spectrum (b) of the light emitted by the laser under 500 MHz pulsed electrical excitation (I_{OFF} = 12.2 mA and I_{ON} = 56.2 mA) and optical injection (P_{inj} = - 14 dBm, $\delta\nu$ = 16 GHz). The injection frequency is indicated by an arrow in (b). 3(c) is a zoom of 3(b).

It is at this point where the role of the optical injection becomes crucial. Figure 3 illustrates this role for specific optical injection conditions. We used same electrical driving conditions as in Fig. 2(g) and injected an optical power P_{inj} = -14 dBm at a detuning $\delta\nu = \nu_{ML} - \nu_{SL}$ = 16 GHz, defined as the frequency difference between the emission frequencies of the ML and the SL in CW conditions. In this case, although the FWHM of the optical pulses (Δt = 40 ps)(Fig. 3(a)) is the same as the width achieved without OI (Fig. 2(h)), an extremely broad and flat OFC is obtained as shown in Fig. 3(b), in contrast with the unresolved spectrum of Fig. 2(i). The CNR is 37 dB and δf_{10} is 54 GHz (corresponding to 108 lines), a factor 12 higher than that of the best OFC obtained at this frequency with sinusoidal excitation. Furthermore, the flatness reaches 54 tones at 3 dB instead of the 3 tones observed in the case of sinusoidal excitation, without optical injection. The measured linewidth of each individual tone is ~ 10 MHz, limited by the BOSA resolution (Fig. 3(c)). However, the real linewidth is expected to be close to 75 kHz, the linewidth of the ML. This is expected based on experimental evidences of a transfer of the linewidth to the SL tones close to the injection frequency, as reported for the OFC generated by GS at higher repetition rates [11, 21], although some broadening cannot be ruled out for far apart tones. In addition to the dynamic chirp in the fast GS process, the origin of the high quality of this broad OFC is the optical injection. Now the externally injected photons are acting as a seed out of which the GS pulses grow during the switch on periods, thus providing a common phase and resulting therefore in a coherent emission. The injected power and the detuning influence the spectral characteristics of the injected OFCs in a complex manner showing similar trends as in the case of sinusoidal gain-switching at higher frequencies [11]. In particular, for maximizing the beneficial effects of the OI in terms of CNR, δf_{10} and flatness, the injected frequency of Fig. 3 has been chosen in the central region of the unresolved non-injected spectrum (Fig. 2(i)), but closer to the low intensity side of this asymmetric spectrum, thus compensating for this asymmetry.

In addition, a suitable choice of optical injection conditions could increase the potential of the generated combs for dual comb spectroscopy by avoiding the requirement of an acousto-optic modulator as shown in reference [24].

We have studied the influence of the pulsed injection conditions on the properties of the 500 MHz GS pulses and the corresponding OFCs. The evolution of the FWHM optical pulse width Δt, δf_{10}, and CNR as a function of the electrical excitation width τ_{elec}, for constant I_{OFF} = 12.2 mA and different values of I_{ON}, is shown in Figs. 4(a)-4(c), respectively. The optical pulses are narrower for higher excitation amplitude. At constant excitation voltage, the evolution of Δt as a function of the excitation pulse width shows a minimum lying at lower excitation width for higher excitation amplitude (Fig. 4(a)). These results are expected from the well known properties of the GS pulses generated under sinusoidal excitation [25]. In this case, at constant repetition frequency, the width of the optical pulses decreases as the amplitude of the excitation signal increases [12, 26, 27]. The decreasing is due to the faster growth of the carrier density that provides the gain needed to build-up the optical pulse and reaches a lower limit related to the photon lifetime [28]. This is also observed in our case where the narrowest pulses are obtained for the highest excitation amplitudes. We attribute the minimum value of Δt as a function of τ_{elec} to two counteracting effects: On one hand, when τ_{elec} decreases the amount of charge injected into the laser decreases as well. Therefore, the accumulated carrier density and the corresponding gain giving rise to the onset of the optical pulse also decrease and consequently, the rise up of the internal photon density becomes slower. But on the other hand, when τ_{elec} increases, the time to switch off the laser also increases and therefore the optical pulses are wider. The minimum shifts towards lower τ_{elec} when increasing the excitation amplitude due to the faster growth of the carrier density that reduces the switching-on time.

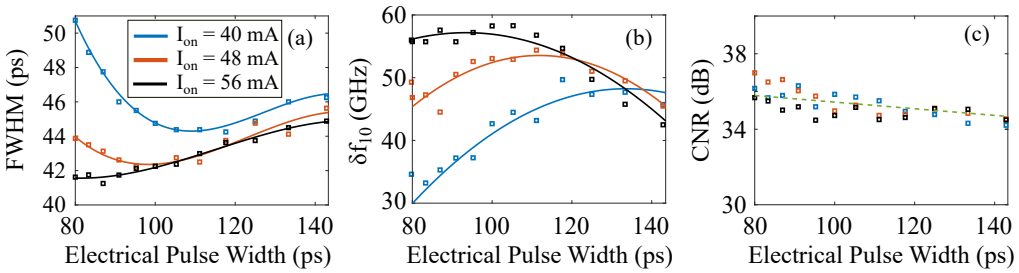

Fig. 4. Evolution of the FWHM of the optical pulse Δt, δf_{10} and CNR, as a function of the electric pulse width τ_{elec} at f_R = 500 MHz, I_{OFF} = 12.2 mA, P_{inj} = - 14 dBm, $\delta\nu$ = 16 GHz and different values of I_{ON}. The lines are drawn as a guide to the eye.

The evolution of δf_{10} as a function of τ_{elec} (Fig. 4(b)) is similar, but opposite, to that of the optical pulse width Δt. An inverse dependence of δf_{10} on Δt is expected in short optical pulses, but δf_{10} also depends on the amplitude of the frequency chirp in the optical pulse. It is clear that the broadest OFCs are obtained at the highest excitation amplitude at τ_{elec} ~ 90-100 ps, which also produces the shortest optical pulses and the maximum chirp. δf_{10} vs. τ_{elec} shows a maximum at a value of τ_{elec} corresponding to the minimum value of Δt. The CNR of the OFCs is high (> 34 dB) for all electrical injection conditions (Fig. 4(c)), and it does not show a clear dependence neither on τ_{elec} nor on the excitation amplitude.

We have also investigated the generation of OFCs at lower repetition frequencies, which would be useful in applications requiring a higher number of tones in the comb. We have observed that at fixed electrical and optical injection conditions the quality of the OFCs degrades when decreasing the repetition rate. The peak arising from the injected optical power becomes higher than the amplitude of the comb tones, which we attribute to the longer time that the laser remains

Optics EXPRESS

switched-off. However, if the electric and optical injection conditions are optimized, high quality OFCs can be generated at lower repetition rates. The optimization procedure consist in selecting switching conditions leading to a non-injected broad and incoherent spectrum as in Fig. 2(i) and then, selecting an injection frequency in the central region of the spectrum but slightly shifted to the low intensity side of the asymmetric spectrum. The injected power should be as low as required for equalizing the spectrum and high enough for ensuring optical locking. Figure 5 shows, as an example, the optical pulse profile (Fig. 5(a)), the corresponding spectrum (Fig. 5(b)) and a zoom of the spectrum (Fig. 5(c)) generated at a repetition frequency of 100 MHz. The duration of the electrical excitation pulse is 100 ps with I_{OFF} = 6.5 mA and I_{ON} = 156.5 mA (achieved by an additional electrical amplification stage).

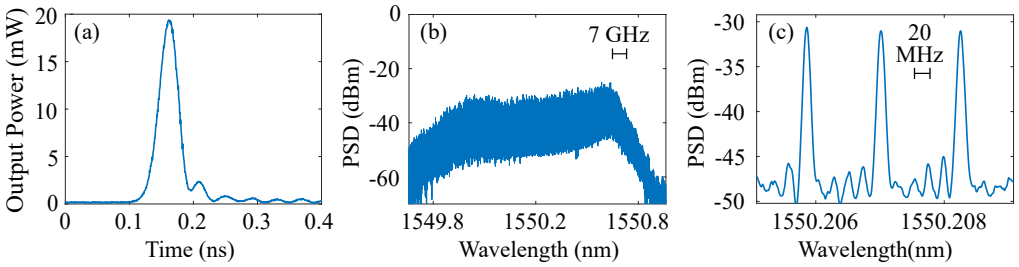

Fig. 5. Temporal trace of the output power (a) and optical spectrum (b) of the light emitted by the laser under 100 MHz pulsed electrical excitation, I_{OFF} = 6.5 mA, I_{ON} = 156.5 mA and optical injection (P_{inj} = - 30 dBm, and detuning, $\delta\nu$ = 16 GHz). 5(c) is a zoom of 5(b).

The injected power has been reduced to -30 dBm and the detuning is 17 GHz. In this case, and due to the lower average output power, the pulses were measured after optical amplification with an Erbium doped fiber amplifier. The pulses are short ($\Delta t \sim$ 34 ps) and exhibit several relaxation oscillations. The OFC is very broad (δf_{10} = 86.4 GHz, corresponding to 866 tones), and its CNR value is 18 dB. OFCs at frequencies lower than 100 MHz were also achieved with these techniques, but a low CNR was measured, probably due to the limit imposed by the BOSA resolution.

Finally, although the experiments reported here were made for discrete mode lasers, the improvement of the comb quality by the combination of pulsed driving conditions and optical injection is expected to be similar in other single-frequency semiconductor laser, such as DFBs or VCSELs.

4. Conclusion

We have experimentally demonstrated that very broad and flat OFCs can be generated from a gain switched semiconductor laser at relatively low frequency by means of pulsed excitation in combination with optical injection. We have studied the role of the switching and injection conditions and have obtained a 10 dB width of 54 GHz (108 lines) at 500 MHz with high CNR. High quality OFCs are also obtained at lower frequencies. These findings may contribute to pave the way not only for the application of combs generated by GS in dual-comb spectroscopy but also for other applications benefiting from the direct generation of relatively wide combs at low frequency without further broadening methods which may spoil the advantages of GS.

Funding

Ministerio de Economia y Competitividad of Spain (TEC201565212-C3-1-P, TEC201565212-C3-2-P); Comunidad de Madrid, European Structural Funds (P2018/NMT-4326); Universidad

Optics EXPRESS

Politécnica de Madrid (Programa propio).

References

1. M. Imran, P. M. Anandarajah, A. Kaszubowska-Anandarajah, N. Sambo, and L. Poti, "A survey of optical carrier generation techniques for terabit capacity elastic optical networks," IEEE Commun. Surv. Tutor **20**, 211–263 (2018).
2. P. J. Delfyett, I. Ozdur, N. Hoghooghi, M. Akbulut, J. Davila-Rodriguez, and S. Bhooplapur, "Advanced Ultrafast Technologies Based on Optical Frequency Combs," IEEE J. Sel. Top. Quant. Electron. **18**, 258–274 (2012).
3. V. Torres-Company and A. M. Weiner, "Optical frequency comb technology for ultra-broadband radio-frequency photonics," Laser Photon. Rev. **8**, 368–393 (2014).
4. T. Shao, R. Zhou, M. D. G. Pascual, P. M. Anandarajah, and L. P. Barry, "Integrated gain switched comb source for 100 gb/s WDM-SSB-DD-OFDM system," J. Light. Technol. **33**, 3525–3532 (2015).
5. M. D. G. Pascual, V. Vujicic, J. Braddell, F. Smyth, P. M. Anandarajah, and L. P. Barry, "InP photonic integrated externally injected gain switched optical frequency comb," Opt. Lett. **42**, 555–558 (2017).
6. M. D. G. Pascual, V. Vujicic, J. Braddell, F. Smyth, P. Anandarajah, and L. Barry, "Photonic Integrated Gain Switched Optical Frequency Comb for Spectrally Efficient Optical Transmission Systems," IEEE Photon. J. **9**, 1–8 (2017).
7. J. Pfeifle, V. Vujicic, R. T. Watts, P. C. Schindler, C. Weimann, R. Zhou, W. Freude, L. P. Barry, and C. Koos, "Flexible terabit/s Nyquist-WDM super-channels using a gain-switched comb source," Opt. Express **23**, 724–738 (2015).
8. A. R. Criado, C. de Dios, E. Prior, G. H. Dohler, S. Preu, S. Malzer, H. Lu, A. C. Gossard, and P. Acedo, "Continuous-wave sub-THz photonic generation with ultra-narrow linewidth, ultra-high resolution, full frequency range coverage and high long-term frequency stability," IEEE Trans. THz Sci. Technol. **3**, 461–471 (2013).
9. B. Jerez, P. Martín-Mateos, E. Prior, C. de Dios, and P. Acedo, "Dual optical frequency comb architecture with capabilities from visible to mid-infrared," Opt. Express **24**, 14986–14994 (2016).
10. S. Chandran, S. Mahon, A. A. Ruth, J. Braddell, and M. D. Gutiérrez, "Cavity-enhanced absorption detection of H_2S in the near-infrared using a gain-switched frequency comb laser," Appl. Phys. B **124**, 63 (2018).
11. A. Rosado, A. Pérez-Serrano, J. M. G. Tijero, Á. Valle, L. Pesquera, and I. Esquivias, "Experimental study of optical frequency comb generation in gain-switched semiconductor lasers," Opt. Laser. Technol. **108**, 542–550 (2018).
12. P. Paulus, R. Langenhorst, and D. Jager, "Generation and optimum control of picosecond optical pulses from gain-switched semiconductor lasers," IEEE J. Quantum Electron. **24**, 1519–1523 (1988).
13. S. Chen, A. Sato, T. Ito, M. Yoshita, H. Akiyama, and H. Yokoyama, "Sub-5-ps optical pulse generation from a 1.55-μm distributed-feedback laser diode with nanosecond electric pulse excitation and spectral filtering," Opt. Express **20**, 24843–24849 (2012).
14. C. Lin, P. Liu, T. Damen, D. Eilenberger, and R. Hartman, "Simple picosecond pulse generation scheme for injection lasers," Electron. Lett. **16**, 600–602 (1980).
15. A. M. Heidt, Z. Li, J. Sahu, P. C. Shardlow, M. Becker, M. Rothhardt, M. Ibsen, R. Phelan, B. Kelly, S. U. Alam, and D. J. Richardson, "100 kW peak power picosecond thulium-doped fiber amplifier system seeded by a gain-switched diode laser at 2 μm," Opt. Lett. **38**, 1615–1617 (2013).
16. D. Bimberg, K. Ketterer, E. H. Böttchër, and E. Scöll, "Gain modulation of unbiased semiconductor lasers: ultrashort light-pulse generation in the 0.8 μm-1.3 μm wavelength range," Int. J. Electron. **60**, 23–45 (1986).
17. S. M. Riecke, H. Wenzel, S. Schwertfeger, K. Lauritsen, K. Paschke, R. Erdmann, and G. Erbert, "Picosecond spectral dynamics of gain-switched DFB lasers," IEEE J. Quantum Electron. **47**, 715–722 (2011).
18. M. Nakazawa, K. Suzuki, and E. Yamada, "Femtosecond optical pulse generation using a distributed-feedback laser diode," Electron. Lett. **26**, 2038–2040 (1990).
19. S. P. O Duill, R. Zhou, P. M. Anandarajah, and L. P. Barry, "Analytical Approach to Assess the Impact of Pulse-to-Pulse Phase Coherence of Optical Frequency Combs," IEEE J. Quantum Electron. **51**, 1–8 (2015).
20. P. M. Anandarajah, R. Maher, Y. Q. Xu, S. Latkowski, J. O'Carroll, S. G. Murdoch, R. Phelan, J. O'Gorman, and L. P. Barry, "Generation of Coherent Multicarrier Signals by Gain Switching of Discrete Mode Lasers," IEEE Photon. J. **3**, 112–122 (2011).
21. R. Zhou, T. N. Huynh, V. Vujicic, P. M. Anandarajah, and L. P. Barry, "Phase noise analysis of injected gain switched comb source for coherent communications," Opt. Express **22**, 8120–8125 (2014).
22. H. Zhu, R. Wang, T. Pu, P. Xiang, J. Zheng, and T. Fang, "A novel approach for generating flat optical frequency comb based on externally injected gain-switching distributed feedback semiconductor laser," Laser Phys. Lett. **14**, 026201 (2017).
23. P. Anandarajah, P. Perry, C. Herbert, D. Jones, A. Kaszubowska-Anandarajah, L. Barry, B. Kelly, J. O'Carroll, J. O'Gorman, M. Rensing, and R. Phelan, "Discrete mode lasers for communication applications," IET Optoelectron. **3**, 1–17 (2009).
24. B. Jerez, P. Martín-Mateos, E. Prior, C. de Dios, and P. Acedo, "Gain-switching injection-locked dual optical frequency combs: characterization and optimization," Opt. Lett. **41**, 4293–4296 (2016).
25. P. P. Vasil'ev, I. H. White, and J. Gowar, "Fast phenomena in semiconductor lasers," Rep. Prog. Phys. **63**, 1997–2042 (2000).
26. W. Zheng and G. W. Taylor, "Gain-switched pulse response of quantum-well lasers," IEEE J. Quantum Electron. **44**, 966–975 (2008).

Optics EXPRESS

27. A. Consoli, I. Esquivias, F. L. Hernandéz, J. Mulet, and S. Balle, "Characterization of gain-switched pulses from 1.55-μm vcsel," IEEE Photon. Technol. Lett. **22**, 772–774 (2010).
28. K. Y. Lau, "Gain switching of semiconductor injection lasers," Appl. Phys. Lett. **52**, 257–259 (1988).

193.144.198.195 {ts '2020-03-11 14:28:54'}